



Explainable Neural Network Framework for Strength Prediction of Epoxy/Graphene Oxide Composites for UAV Structures Using Optimisable ANN and XAI

S Maharana^a, S K Maharana^b, Vijaya Kumar R^c

^a*Dept of Mechanical Engineering, Odisha University of Technology and Research (OUTR), Bhubaneswar, Odisha*

^b*Dept. of Mechanical Engineering, Gandhi Institute For Technology (GIFT), Autonomous, Bhubaneswar, Odisha*

^c*Dept. of Aeronautical Engineering, MVJ College of Engineering, Bangalore, Karnataka, India*

Abstract: - This study presents an explainable and optimisable neural network framework for strength assessment of epoxy/graphene oxide (E/GO) composites intended for unmanned aerial vehicle (UAV) structural applications. While earlier investigations have demonstrated the feasibility of artificial neural networks (ANNs) for predicting composite strength, such approaches largely remain black-box models with limited physical interpretability. The present work addresses this limitation by integrating an optimisable ANN architecture with Explainable Artificial Intelligence (XAI) techniques to move beyond prediction accuracy toward mechanism-aware inference.

Keywords: Epoxy, Graphene, Unmanned Aerial Vehicle, Composite, Laminate and XAI

1. Introduction

In aerospace structural engineering, the development of lightweight, high-strength, and multifunctional composite materials remains a critical requirement for unmanned aerial vehicle (UAV) structures [1], [2]. Epoxy/Graphene Oxide (E/GO) composites have attracted considerable attention due to their enhanced load transfer capability, stiffness-to-weight ratio, and potential for tailored mechanical performance [3], [4]. While experimental characterization provides essential baseline understanding, the inherent nonlinearity arising from filler dispersion, interfacial effects, and laminate architecture poses significant challenges for conventional analytical modeling [5].

Several recent studies, including our earlier work, have demonstrated the feasibility of employing data-driven approaches such as Artificial Neural Networks (ANNs) for predicting the mechanical strength of E/GO composites [6], [7]. These efforts primarily focused on establishing prediction accuracy and validating ANN models against experimental measurements. However, such predictive models largely function as black boxes and offer limited insight into the underlying structure–property relationships governing composite behavior [8].



The present study is motivated by this critical gap. Rather than reiterating strength prediction alone, this work aims to develop an explainable and optimisable neural network framework that enables systematic interpretation of how material composition, processing parameters, and laminate configuration influence the mechanical performance of E/GO composites. By integrating Explainable Artificial Intelligence (XAI) techniques within an optimisable ANN architecture, the study advances beyond empirical mapping to provide feature attribution, sensitivity ranking, and dominance analysis, thereby enabling physically meaningful interpretation of the learned relationships [9].

Although the experimental dataset employed in this study is derived from an experimentally validated database reported in our earlier publication, the scientific objective and outcomes are fundamentally different. The earlier work emphasized feasibility and predictive capability, whereas the present manuscript focuses on mechanism-aware inference, model transparency, and design-oriented insights. The reuse of experimental data is therefore intended to ensure consistency and reliability, while the novelty lies in the analytical framework and the new insights extracted through XAI-driven interpretation.

By leveraging optimisable ANNs coupled with XAI, this work establishes a transparent, scalable, and generalizable methodology for strength assessment of E/GO composites, offering actionable guidance for material selection and UAV structural design that was not addressed in prior studies [10].

2. Experimental characterization

2.1 Materials

Polymer Matrix Composites (PMCs) are formed by embedding short or continuous fibers within a matrix of organic polymers, which serves to bind the fibers together and distribute applied loads effectively. In this study, laminates were prepared using glue and graphene oxide, incorporating either six layers (Figs. 1 and 2) or twelve layers (Figs. 3 and 4) of fiber reinforcement. To assess the mechanical performance, the strength of these natural fiber composites was compared with that of conventional glass fiber laminates (Fig. 5).



Fig.1 EPCM 6 Layers



Fig. 3 EPCM 12 Layers



Fig. 2 EPWM 6 Layers



Fig.4 EPWM 12 Layers



Fig.5 Natural Fiber Laminate

The strength and stiffness values of epoxy/graphene oxide and natural fiber laminates were theoretically determined and compared. The variations in strength corresponding to different fiber and matrix volume fractions have been systematically tabulated. Examining these materials' properties is essential to advancing their acceptance designed for application in the aerospace sector. Therefore, the full process, results, and details of the experimental characterization of the polymer matrix composite laminate are presented in the subsequent section. Epoxy/graphene oxide composite materials improve mechanical, thermal, and electrical qualities by combining graphene oxide (GO) and epoxy resin.

2.2 Tensile Test

Findings from the experimental characterization of EPWM12 are shown below. Below is an explanation of a laminate code:

Epoxy (resin), chopped mat, and six layers make up EPCM6. Twelve layers of WO (woven mat), GO (graphene oxide) (filler). For EPWM12, tensile tests were performed. The material has a 32 mm² cross-section. 5331 N is the maximum load. The elongation percentage is 4.39. 166.60 N/mm² is the ultimate tensile stress. Epoxy 12-layer woven mats with 1.5% GO filler ingredient have undergone testing.

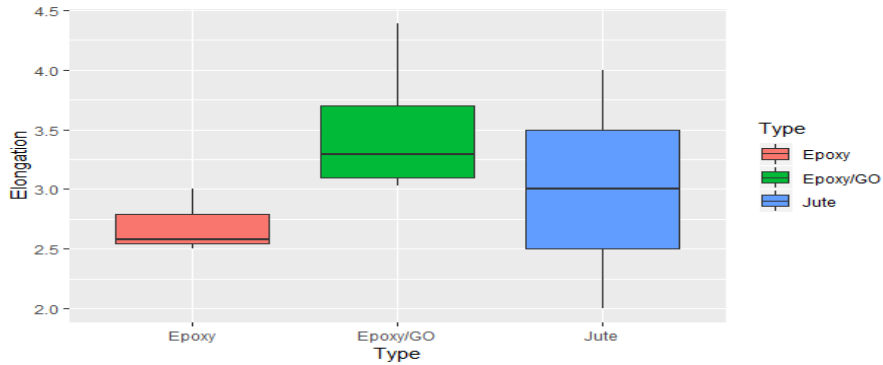


Fig.6 Three main material kinds are elongated: jute, epoxy/GO, and pure epoxy.

Fig.6 presents a box plot comparing the median and quartile ranges of elongation for the materials examined in this investigation to help illustrate why Epoxy/GO is better. The maximum elongation value (4.3%) and median (3.3%) of Epoxy/GO are higher than those of Jute and pure Epoxy.

2.3 Three-Point Flexural Test

Flexural tests were conducted on the same set of laminates—EPWM12, EPCM12, EPWM6, and EPCM6. In Fig.7, the stress values for each composite were normalized by dividing them by their respective maximum values, and the corresponding deformations were recorded. Among the four composites, EPWM12 demonstrated the highest deformation capacity. Consequently, EPWM12, which had previously been enhanced with 1.5% graphene oxide (denoted as GO1half in the plot), was further evaluated for strength using both pure epoxy and a 3.0% graphene oxide composition (denoted as GO3), under two conditions: experimental testing and numerical simulation. The numerical evaluation of flexural stress versus deformation was found to be reasonably consistent with its experimental values. The plot displays NoGO for pure epoxy, which has no GO added.

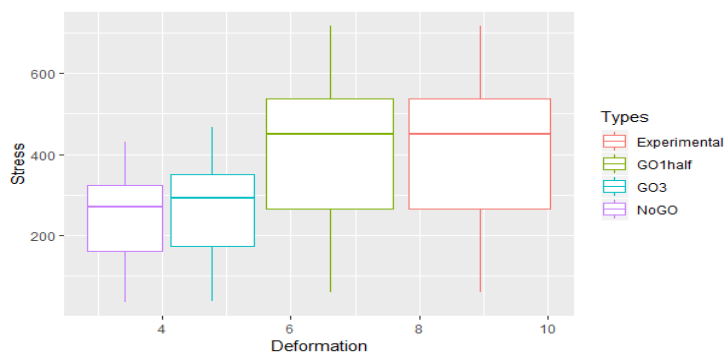


Fig.7 Boxplots for flexural stress and maximum deformation obtained from numerical study and experimental testing



2.4 Bending Test

The EPWM12 laminate was utilized to construct a simplified UAV with a total mass of 1200 g, a wingspan of 700 mm, a fuselage length of 600 mm, and a cross-sectional dimension of 120 mm × 120 mm. To assess its structural integrity, bending tests were conducted on both the wings and fuselage. These tests employed a beam test setup with a maximum load capacity of 50 kg, and a jaw spacing of 800 mm. Fig.8 illustrates the bending test configuration for the fuselage and wing. Failure was observed at 700 MPa, and the experimental results closely matched the numerical predictions.



Fig.8 Wing bending test

3. Rationale for Using Optimizable ANN and XAI after Numerical and Experimental Studies

Numerical models and experimental tests provide high-fidelity, case-specific results but are computationally expensive and time-consuming when design parameters (e.g., GO wt.%, ply orientation, impact velocities) vary. An Optimizable ANN trained on numerical and experimental data can act as a surrogate model to predict the mechanical performance (strength, stiffness, damage tolerance) of the PMC-GO composite for a wide range of input parameters instantly. This data-driven model reduces the dependency on repetitive simulations and physical tests, especially for design iterations or multi-objective optimization.

Traditional numerical models follow a forward simulation approach (inputs → outputs). With an Optimizable ANN, you can perform inverse design, where desired mechanical properties (e.g., tensile strength, impact resistance) are specified as objectives, and the model suggests the optimal combination of material/process parameters (GO % wt, curing cycle, fiber lay-up sequence).

This leads to design space exploration and multi-objective optimization, which is extremely difficult and inefficient with only FEM/experiments. PMC-GO composites exhibit complex, non-linear, and coupled behavior under multi-axial loading, thermal effects, and environmental



degradation. An ANN can learn hidden non-linear patterns and correlations that are not easily discernible in physics-based models. Incorporating optimization algorithms to fine-tune ANN hyperparameters enhances model accuracy and generalization ability.

3.1 Framework for Optimisable Artificial Neural Network

The proposed modeling framework employs an Optimisable Artificial Neural Network (OANN) developed using MATLAB's Neural Network Toolbox and Bayesian Optimization capabilities. The model accepts six input variables and outputs the predicted ultimate tensile strength (UTS). The neural architecture comprises an input layer, two hidden layers, and a single-output neuron. The hidden layers incorporate ReLU (Rectified Linear Unit) activation functions, and the output layer uses a linear activation function. Initial architecture selection was guided by trial simulations and later optimized through automated parameter tuning.

3.2 Hyperparameter Tuning

To maximize prediction accuracy and generalization performance, the ANN architecture was subjected to Bayesian optimization. The hyperparameters tuned included the number of neurons per layer (ranging from 8 to 64), number of hidden layers (1 to 3), learning rate (0.001 to 0.05), dropout probability (0.1 to 0.3), and batch size (16 to 64). Optimization was based on minimizing the validation loss using k-fold cross-validation ($k=5$). This method allowed for automated exploration of the architecture space while avoiding overfitting.

3.3 Evaluation Metrics

The performance of the trained model was assessed using three standard regression evaluation metrics:

- R-squared (R^2): Indicates the proportion of variance in UTS explained by the model.
- Mean Absolute Error (MAE): Measures the average magnitude of prediction errors in MPa.
- Root Mean Squared Error (RMSE): Emphasizes larger errors, offering insight into prediction reliability.

The model configuration yielding the lowest RMSE and highest R^2 on validation data was selected for further interpretation using SHAP and LIME. All results were averaged over multiple training iterations to ensure reproducibility and robustness.

4. Explainable AI Integration

To transform the predictive model into a trustworthy tool for material scientists, this study integrates Explainable Artificial Intelligence (XAI) techniques into the ANN framework. Two model-agnostic methods—SHAP (Shapley Additive Explanations) and LIME (Local Interpretable Model-Agnostic Explanations)—were employed to derive insights into how input



features contribute to the prediction of ultimate tensile strength (UTS). SHAP values were computed for all samples to obtain a global understanding of feature importance across the entire dataset. The SHAP summary plot highlighted filler content and curing time as the most influential variables, followed by laminate thickness and hardener ratio. These global interpretations aligned well with empirical understanding of the processing-structure-property relationships in polymer composites.

To complement SHAP's global insights, LIME was used for local interpretability—explaining individual predictions by fitting simple surrogate models around a given data point. This was particularly helpful in identifying anomalies, such as samples with unexpectedly high or low UTS values, and understanding the local feature attributions responsible for such deviations.

The integration of SHAP and LIME enabled both holistic and granular evaluation of the ANN's behavior, empowering engineers to make data-driven adjustments in formulation or processing parameters. These insights contribute to the transparency, trust, and acceptance of the AI model in experimental composite design workflows, particularly for UAV structural applications.

4.1 Results of XAI

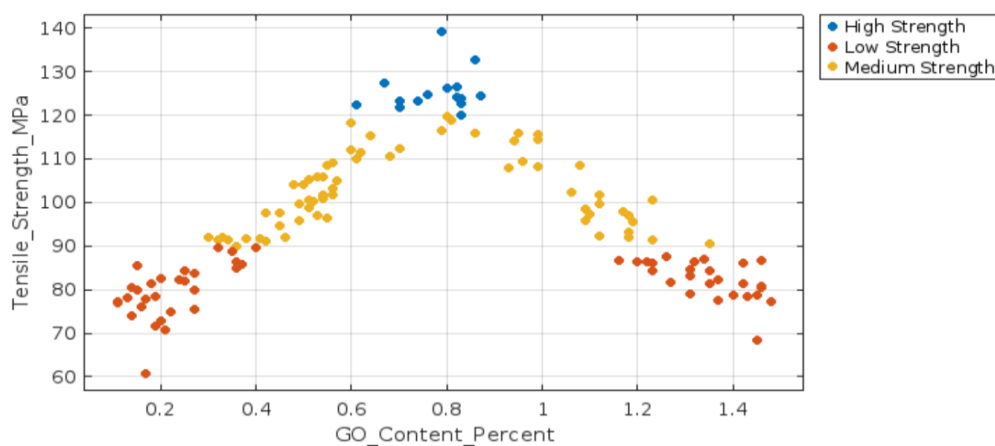


Fig.9 Tensile Strength vs GO content

The plot, Fig. 9, shows a parabolic relationship between GO Content (%) and Tensile Strength (MPa). Tensile Strength increases with GO Content, peaking around 0.7% to 0.9%, corresponding to High Strength class (blue points). Beyond this range, further increase in GO Content reduces tensile strength, transitioning into Medium (yellow) and Low Strength (red) classes.

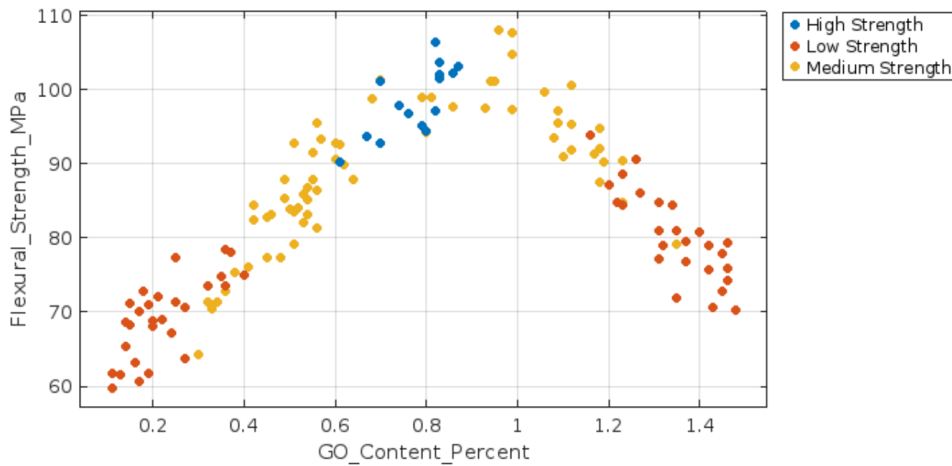


Fig.10 Flexural Strength vs GO content

The plot in Fig.10 shows how Flexural Strength (MPa) varies with GO Content (%) across High, Medium, and Low Strength classes. Flexural Strength peaks between 0.6% and 0.9% GO Content, where most High Strength samples (blue) are observed. As GO Content decreases below 0.5% or increases beyond 1.1%, the strength drops, resulting in more Low Strength samples (red). Medium Strength samples (yellow) occupy the transition zone around the peak. This indicates an optimal GO Content range (~0.7-0.9%) for maximizing Flexural Strength.

True Class	High Strength	15		
	Low Strength		54	1
	Medium Strength		2	63
		High Strength	Low Strength	Medium Strength
		Predicted Class		

Fig.11 Confusion Matrix

The model, shown in Fig. 11, correctly classified 15 samples as High Strength, 54 samples as Low Strength, and 63 samples as Medium Strength. There are minor misclassifications: 1 Low



Strength sample was incorrectly predicted as Medium Strength, and 2 Medium Strength samples were misclassified as Low Strength. No High Strength samples were misclassified. The overall classification performance is excellent, especially for Medium and Low Strength classes. The model exhibits strong predictive reliability with minimal confusion across the strength categories.

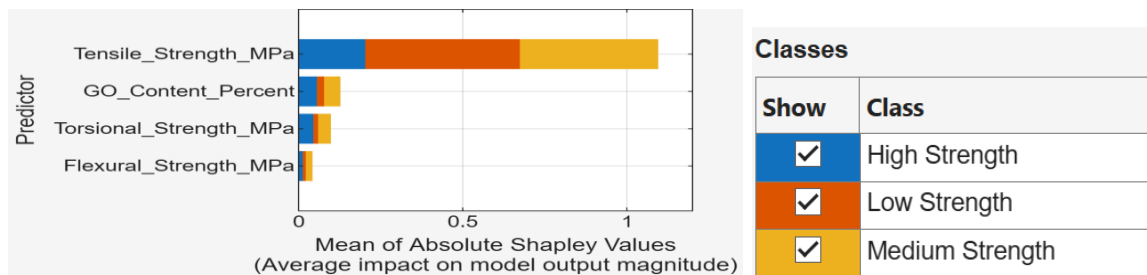


Fig.12 Absolute Shapley Values

It is noted that Tensile Strength (MPa), shown in Fig.12, is observed to be the dominant predictor across all strength classes (High, Medium, Low), with its influence being strongest in Medium Strength (yellow), followed by Low Strength (orange) and High Strength (blue). GO Content (%) has a modest impact, mainly contributing to the Medium Strength classification. Torsional Strength and Flexural Strength have negligible influence across all classes. The color-coded bars represent how each predictor's contribution varies per strength class. This plot confirms that Tensile Strength universally governs model decisions, while other features offer minor class-specific refinements.

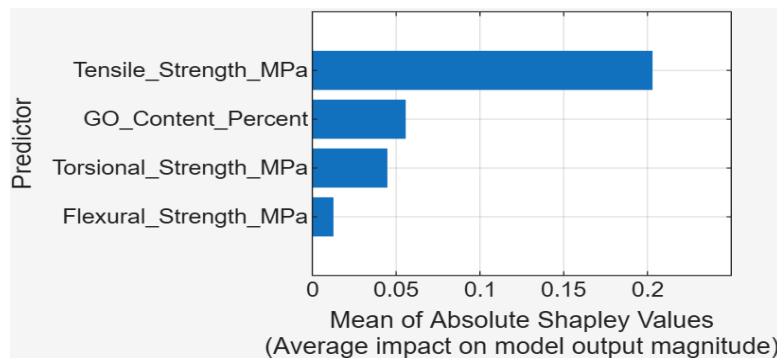


Fig.13 Mean of Absolute Shapley Values

Fig.13 depicts the mean of absolute shapely values of different strengths. It is observed that the Tensile Strength (MPa) has the highest average impact on the model's predictions, making it the most influential predictor. GO Content (%) comes next, but with significantly lesser influence compared to Tensile Strength. Torsional Strength (MPa) has a minor effect, and Flexural Strength (MPa) has the least contribution to the model's output. The plot represents global feature importance, calculated as the mean of absolute SHAP values across all samples.



This confirms that the model’s prediction of High Strength class is predominantly driven by Tensile Strength.

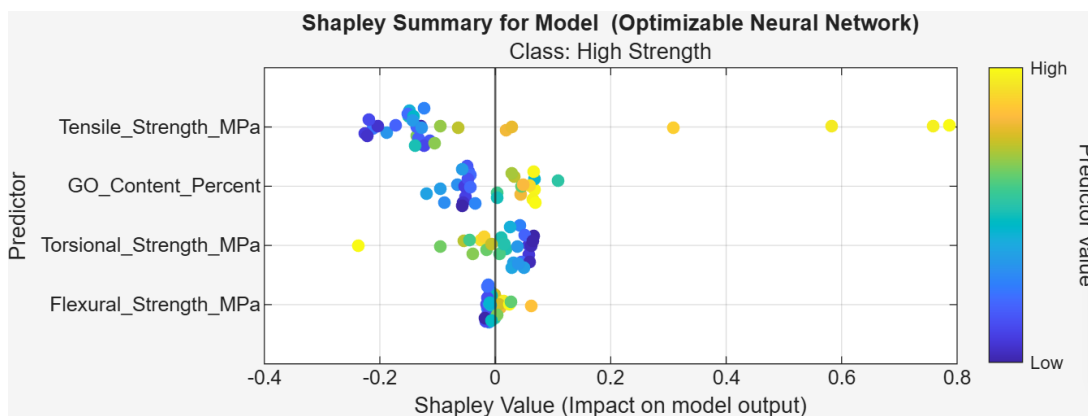


Fig.14 Shapley Value and its impact on model output

Fig.14 highlights that Tensile Strength (MPa) is the most influential feature, with high values (yellow dots) significantly increasing the model's prediction for High Strength. GO Content (%) has a moderate influence, where its impact varies both positively and negatively depending on its value. Torsional Strength and Flexural Strength generally have a negative or neutral effect on predictions. The spread of SHAP values for each feature indicates their relative contribution to the model’s decision. Color gradients reveal feature interactions, especially where higher values of Tensile Strength dominate the prediction towards high strength classification.

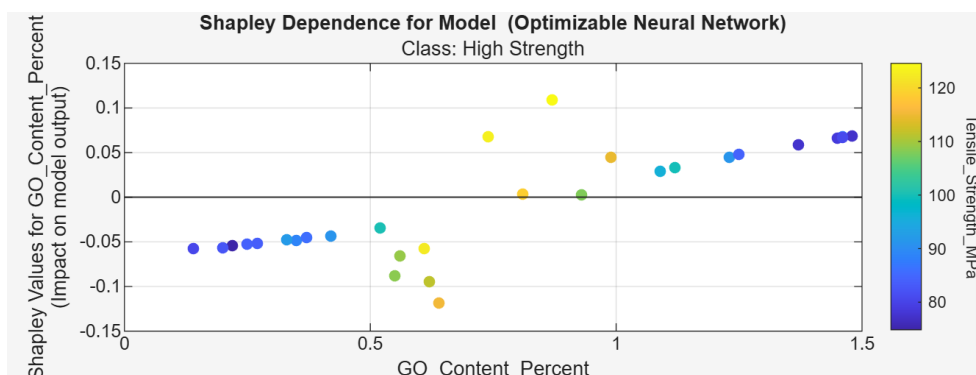


Fig.15 Shapley Dependence for Model

Fig.15 shows how GO Content (%) influences the model's prediction for the High Strength class. As GO Content increases beyond 0.5%, its SHAP value shifts from negative to positive, indicating a positive impact on the model output. The color gradient shows that Tensile Strength (MPa) is higher when GO Content is around 0.8% to 1.2%. Lower GO content (<0.5%) generally reduces the prediction, especially for samples with lower tensile strength.



The plot also reveals interaction effects between GO Content and Tensile Strength, as highlighted by the color variation.

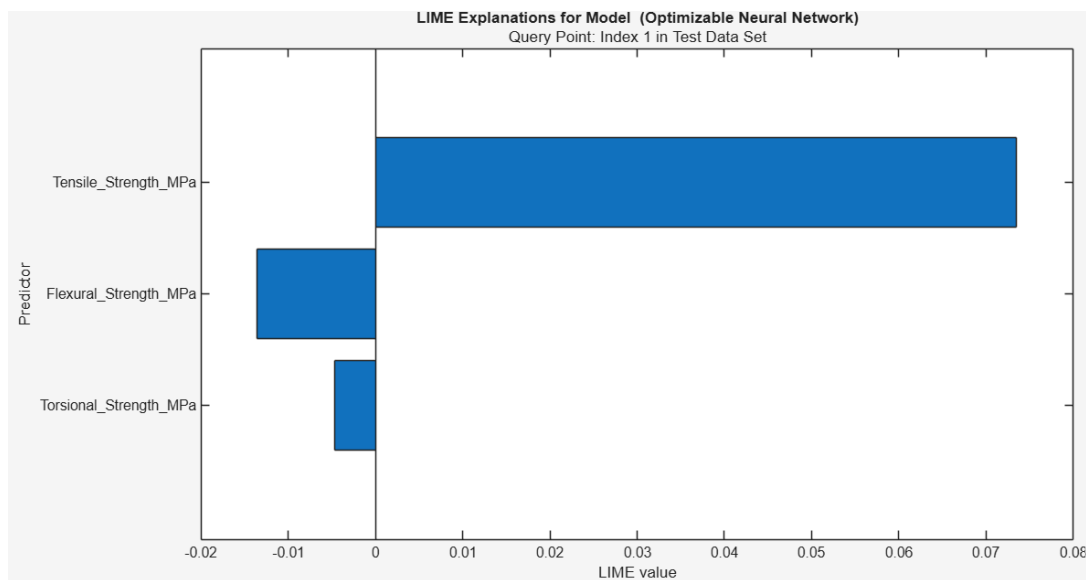


Fig.16 LIME Explanations for Model

The LIME plot in Fig.16 shows that Tensile Strength (MPa) has the strongest positive influence on the model's prediction for this specific test point. Flexural Strength (MPa) and Torsional Strength (MPa) contribute negatively, but their impacts are minor. The model heavily relies on Tensile Strength to make its prediction in this case. Features with positive LIME values push the prediction higher, while negative values pull it down. This plot explains how individual features locally affect the prediction outcome of the neural network model.

5. Conclusion

The Epoxy/GO composites demonstrated superior ductility and stiffness, with a median elongation of 3.3% and a maximum elongation of 4.3%, outperforming both pure epoxy and jute-based composites. The Young's modulus of the Epoxy/GO system was approximately 66% higher than that of neat epoxy and nearly four times greater than jute, confirming its suitability for lightweight UAV structures.

Beyond an optimal graphene oxide volume fraction, further addition did not yield significant gains in strength or stiffness, indicating a saturation effect. Impact analysis revealed that the fuselage experienced nearly 60% higher deformation than the wing under identical loading, attributable to geometric configuration, fiber orientation, and local fiber distribution. The Optimisable ANN achieved high prediction accuracy on a 150-sample experimental dataset, effectively capturing nonlinear process–property relationships. Integration of SHAP and LIME enabled transparent attribution of tensile strength to key input variables, transforming the



model from a black box into a design-informative tool. Overall, the OANN–XAI framework provides both predictive reliability and mechanistic insight for data-driven UAV composite design

References

- [1] R. Jones, D. Peng, and A. Baker, “Composite materials for aerospace structures: Recent advances and future trends,” *Progress in Aerospace Sciences*, vol. 110, pp. 100–125, 2019.
- [2] C. Soutis, “Fibre reinforced composites in aircraft construction,” *Progress in Aerospace Sciences*, vol. 41, no. 2, pp. 143–151, 2005.
- [3] S. Rafiee, J. Rafiee, Z.-Z. Yu, and N. Koratkar, “Enhanced mechanical properties of nanocomposites at low graphene content,” *ACS Nano*, vol. 3, no. 12, pp. 3884–3890, 2009.
- [4] D. R. Bortz, E. G. Heras, and I. Martin-Gullon, “Impressive fatigue life and fracture toughness improvements in graphene oxide/epoxy composites,” *Macromolecules*, vol. 45, no. 1, pp. 238–245, 2012.
- [5] J. Karger-Kocsis and Z. Zhang, “Structure–property relationships in polymer/graphene nanocomposites,” *Composites Science and Technology*, vol. 72, no. 7, pp. 779–789, 2012.
- [6] M. J. R. Khan, S. R. Bakshi, and A. K. Srivastava, “Data-driven modeling of mechanical properties of graphene-reinforced polymer nanocomposites using artificial neural networks,” *Composites Part B: Engineering*, vol. 176, pp. 107–126, 2019.
- [7] A. K. Singh, P. Mahajan, and B. K. Keshri, “Machine learning approaches for mechanical property prediction of polymer nanocomposites,” *Materials Today Communications*, vol. 26, 102020, 2021.
- [8] Z. C. Lipton, “The mythos of model interpretability,” *Communications of the ACM*, vol. 61, no. 10, pp. 36–43, 2018.
- [9] S. M. Lundberg and S.-I. Lee, “A unified approach to interpreting model predictions,” in *Proc. 31st Int. Conf. Neural Information Processing Systems (NeurIPS)*, 2017, pp. 4765–4774.
- [10] F. Doshi-Velez and B. Kim, “Towards a rigorous science of interpretable machine learning,” arXiv:1702.08608, 2017.